

## DETECTION OF GASEOUS COMPOUNDS WITH DIFFERENT TECHNIQUES

**Janusz Mikołajczyk<sup>1)</sup>, Zbigniew Bielecki<sup>1)</sup>, Tadeusz Stacewicz<sup>2)</sup>, Janusz Smulko<sup>3)</sup>,  
Jacek Wojtas<sup>1)</sup>, Dariusz Szabra<sup>1)</sup>, Łukasz Lentka<sup>3)</sup>, Artur Prokopiuk<sup>1)</sup>, Paweł Magryta<sup>2)</sup>**

1) Military University of Technology, Institute of Optoelectronics, Kaliskiego 2, 00-908 Warsaw, Poland

(✉ janusz.mikolajczyk@wat.edu.pl, +48 26 183 9430, zbielecki@wat.edu.pl, jacek.wojtas@wat.edu.pl, dariusz.szabra@wat.edu.pl, artur.prokopiuk@wat.edu.pl)

2) University of Warsaw, Faculty of Physics, Pasteura 5, 02-093 Warsaw, Poland

(Tadeusz.Stacewicz@fuw.edu.pl, Pawel.Magryta@fuw.edu.pl)

3) Gdańsk University of Technology, Faculty of Electronics, Telecommunications and Informatics, G. Narutowicza 11/12, 80-233 Gdańsk, Poland (jsmulko@eti.pg.gda.pl, lukasz.lentka@gmail.com)

### Abstract

Sensing technology has been developed for detection of gases in some environmental, industrial, medical, and scientific applications. The main tasks of these works is to enhance performance of gas sensors taking into account their different applicability and scenarios of operation. This paper presents the descriptions, comparison and recent progress in some existing gas sensing technologies. Detailed introduction to optical sensing methods is presented. In a general way, other kinds of various sensors, such as catalytic, thermal conductivity, electrochemical, semiconductor and surface acoustic wave ones, are also presented. Furthermore, this paper focuses on performance of the optical method in detecting biomarkers in the exhaled air. There are discussed some examination results of the constructed devices. The devices operated on the basis of enhanced cavity and wavelength modulation spectroscopies. The experimental data used for analyzing applicability of these different sensing technologies in medical screening. Several suggestions related to future development are also discussed.

Keywords: gas sensors, laser absorption spectroscopy, CEAS, MUPASS, breath analyses, medical screening.

© 2016 Polish Academy of Sciences. All rights reserved

## 1. Introduction

The gas detection is very important in many applications. It is particularly important in the petrochemical industry (to detect toxic gases), in the measurement of key species in the production and processing technology (to control dynamic changes), as well as in the environment protection (to determine profiles of greenhouse gases). Additionally, more attention is focused on the ability to detect vapors of explosives in the security activities [1]. At present, many gas sensors are also tested for medical analyses of gases contained in a patient's breath in searching disease biomarkers. Such gases may be nitric oxide, carbon monoxide, methane, and many more. The analytical study of gases is normally performed using the laboratory equipment such as chromatographs or small low-cost dry devices as pellistors, semiconductor sensors, or electrochemical devices. In addition to these techniques, there are developed other methods with new capabilities. The characteristics of chosen techniques are summarized in Table 1.

In this paper, commonly used techniques in gas sensing are described. The main part of this review deals with optical devices. These include the *Non-Dispersive Infrared* sensors, *Tunable Diode Laser Absorption Spectroscopy*, *Wavelength Modulation Spectroscopy*, *Differential Optical Absorption Spectroscopy*, *Light Detection and Ranging and Absorption Spectroscopy* *Photoacoustic Spectroscopy*, *Fourier Transform Infrared* spectrometry and *Cavity Ring-Down Spectroscopy* absorption.

Table 1. Characteristics of some gas sensor technologies [2, 3].

METHOD	ADVANTAGES	DISADVANTAGES
Optical spectroscopy	<ul style="list-style-type: none"> <li>• direct and rapid,</li> <li>• selective with good sensitivity</li> <li>• minimal drift and high gas specificity,</li> <li>• zero cross-response to other gases.</li> </ul>	<ul style="list-style-type: none"> <li>• determination of significant and distinct spectral region of analyses.</li> </ul>
Gas chromatography	<ul style="list-style-type: none"> <li>• very accurate and highly selective.</li> </ul>	<ul style="list-style-type: none"> <li>• not easy to use on-line,</li> <li>• gas sampling necessary,</li> <li>• very expensive.</li> </ul>
Semiconductor	<ul style="list-style-type: none"> <li>• low cost,</li> <li>• measure total exposure over time,</li> <li>• highly sensitive at the low ppm (<i>parts per million</i>) level</li> </ul>	<ul style="list-style-type: none"> <li>• poisoning can occur,</li> <li>• exhibit non-reversible behaviour,</li> <li>• may consume analyse,</li> <li>• drift and cross-respond to other gases,</li> <li>• change with humidity levels.</li> </ul>
Catalytic (Pellistor gas sensors)	<ul style="list-style-type: none"> <li>• low cost,</li> <li>• presence detection of flammable gases.</li> </ul>	<ul style="list-style-type: none"> <li>• poisoning can occur,</li> <li>• sensitive to groups of gases,</li> <li>• errors in presence of other flammable gases,</li> <li>• suffer from zero drift at ppm levels.</li> </ul>

In the experimental section, an optoelectronic sensor for detection of three trace gas species in human breath (biomarkers) is described. These sensors have been designed within the frame of the “Sensormed” Project financially supported by Polish National Centre of Research and Development. The obtained results show that the sensor’s detection limits are sufficient for nitric oxide, carbon monoxide and methane monitoring in human breath for both sick and healthy man. These advantages may indicate substantial progress in early diagnosis of diseases due to application of equipment for fast medical screening.

## 2. Different gas sensor technologies

For many years, numerous sensor technologies have been developed for detection of different compounds. Application of high sensitivity gas sensors is widespread in the gas diagnosis, for instance to evaluate different noxious species, to detect various biomarkers in breath or to search trace amounts of explosives [4]. Detecting methods are dominated by mass spectrometry, chromatography, catalytic sensors, thermal conductivity sensors, semiconductor sensors, electrochemical devices or acoustic sensors [5]. The performance characteristics of sensors are based on some properties including their sensitivity, selectivity, detection limit, response time and recovery time.

### 2.1. Catalytic sensors

Catalytic sensors are used for detection of combustible gases. Practically, they are divided into the pellistor and thermoelectric ones. The pellistor-type catalytic gas sensor (Fig. 1) consists of two platinum coils (beads). The active bead ( $R_a$ ) is activated with a catalyst made from a metal (platinum or palladium), whereas the second bead (the inactive one –  $R_i$ ) has no catalyst and acts as the reference element. The concentrations of combustible compounds can be detected by monitoring the change of platinum resistance resulting from the temperature increase [6].

A rise of temperature occurs due to catalytic oxidation of the combustible compounds. That increases the coil resistance  $R_a$  and causes a voltage imbalance at Wheatstone bridge output.



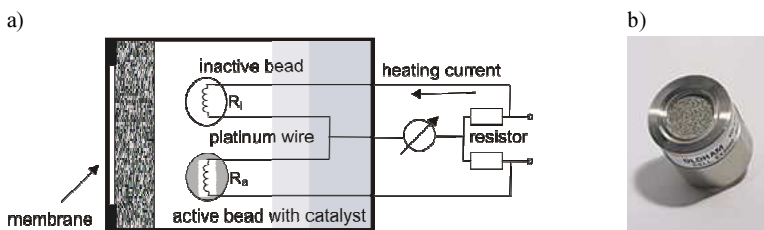


Fig. 1. A scheme of: a) the pellistor-type gas sensor; b) a sensor with sintered port [7].

The thermoelectric gas sensor is a transducer converting – using the Seebeck effect – the temperature change to an electric signal, due to the heat reaction between a catalyst and gas species [8]. This effect can be used to develop a thermal sensor by placing the hot junction on a thermally isolated structure like a membrane, bridge, *etc.*, and the cold junction on the bulk chip (Fig. 2a). The membrane structure supporting the hot junctions is covered with a chemically active layer producing heat resulting from its interaction with an analyte. Several thermocouples are connected in series in order to achieve a higher sensitivity; then the heat losses to the substrate made of a thermoelectric material are also reduced. Fig. 2b shows a scheme of CMOS-based thermopile consisting of a dielectric membrane and aluminum/polysilicon thermocouples [9]. The Seebeck coefficient is equal to 111 mV/K. It can be used to detect different gases by simply changing the catalytic materials employed in the device. This sensor does not require an external power supply because it measures the voltage difference between the hot and cold junctions. Additionally, it shows good linearity with respect to the sample gas concentration. For instance, the acetone detection limit for such sensors with a chromium metal catalyst is as low as 28 ppm [10].

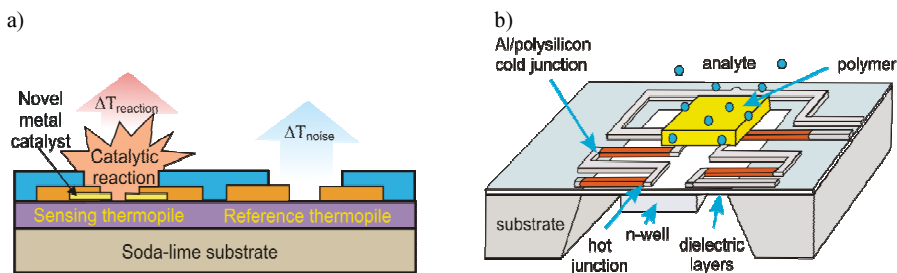


Fig. 2. The thermoelectric sensor: a) the concept of operation; b) a schematic.

## 2.2. Thermal Conductivity (TCD) gas sensors

TCD sensors are based on heat transmission in the examined gas. The thermal conductivity coefficient is measured and compared with one of a known reference sample determined by the identical sensor (Fig. 3a). TDC devices are usually used for detection of gases with large thermal conductivities, like hydrogen, helium or carbon dioxide [11]. Each sensor contains an extremely sensitive element of low thermal capacity. Fig. 3b shows a profile of the micro-thermal conductivity gas sensor. Its measurement principle is based on a decrease of the effective thermal resistance between the sensitive area (a heated membrane) and the substrate, caused mainly by the thermal conductance of the gas in thin membrane. The heating element is a resistor which is located in the middle of the membrane.

The gas detection based on the thermal conductivity is widely used in automotive industry as well as in medical and environmental monitoring systems [12]. TDC sensors are especially suitable in safety applications, for example in hydrogen cells, where a leakage of H<sub>2</sub> must be



detected before its concentration reaches the explosive limit (4% in the air) [13]. The device gives a fast response, due to its small size and low mass.

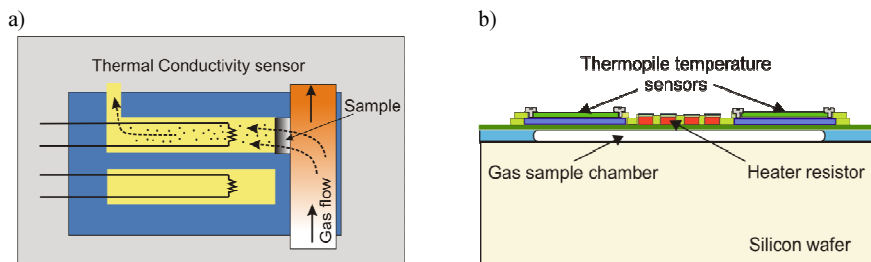


Fig. 3. The thermal conductivity sensor: a) the concept of operation; b) an example of micro-thermal conductivity gas sensor.

### 2.3. Electrochemical gas sensors

Electrochemical sensors measure the concentration of a target gas due to its oxidation or reduction at an electrode. As a result a current occurs which is proportional to the gas concentration [14]. A typical electrochemical sensor consists of sensing and counter electrodes separated by a thin layer of electrolyte (Fig. 4).

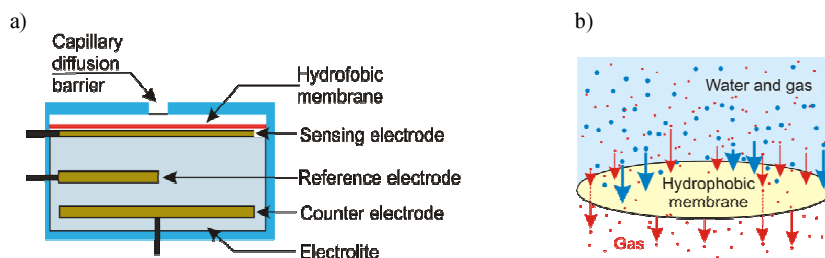


Fig. 4. A scheme of: a) a typical electrochemical sensor; b) operation of a hydrophobic membrane.

The detected gas goes through a thin capillary diffusion barrier and then diffuses through a hydrophobic membrane to the sensing electrode surface. The membrane is used to prevent liquid electrolyte from leaking out and to generate enough electrical signal at the sensing electrode. The reference electrode keeps a stable and constant potential at the sensing electrode. When the gas reaches the sensing electrode, an oxidation or electrochemical reduction occurs, depending on type of the gas. For example, carbon monoxide may be oxidized to carbon dioxide, while oxygen reduction may produce water. An oxidation reaction results in the flow of electrons from the sensing electrode to the counter electrode through the external circuit. For the reduction, the electron flow is reversed. These flows constitute electric currents, which are proportional to the gas concentration. Unfortunately, the cross-sensitivity can cause a practical problem in such sensors by giving similar response in the presence of various gases. In practice, electrochemical sensors are divided into amperometric, potentiometric and conductometric instruments [15]. Electrochemical gas sensors have a limited sensitivity and a relatively high gas detection threshold level but are very reliable and the same sensor can work effectively for several years. Therefore, these sensors can be applied in numerous industrial applications.

Electrochemical gas sensors can contain not only liquid, but also solid electrolyte [16]. The latter solution reduces the risk of leaks. Moreover, an electrochemical sensor, characterized by its current-voltage curve, can make use of its shape determined by the ambient gas. It means that some more advanced detection algorithms can use any difference in the current-voltage curve induced by the ambient gas to improve their gas detection selectivity [17].

## 2.4. Semiconductor gas sensors

Semiconductor gas sensors (metal oxide sensors) are electrical conductivity elements. The DC resistance of their active porous layer changes due to adsorption/desorption processes related to the operating temperature and composition of ambient gas atmosphere. The gas sensors work at elevated temperatures in order to accelerate adsorption/desorption processes and to reduce the effects of temperature instability (Fig. 5). Usually, the active layer consists of a thin metal-oxide film and a heater [18, 19]. Their typical operating temperatures are between 300°C and 900°C, depending on the sensor construction and the detected gas, and can be modulated to improve the gas detection. A heat pulse is often used to cleanse the sensor before gas detection. The gas sensors can be used to determine the composition of combustive gases at relatively high temperatures, but have limited use in the explosive environment. Using these sensors, gases such as ammonia, carbon monoxide, sulfurous gases, nitrogen oxides ( $\text{NO}_x$ ), and hydrocarbons, as well as *Volatile Organic Compounds* (VOCs) can be detected. The measuring range depends on the detected compound, including the values from a few ppb (*parts per billion*) to a percent range.

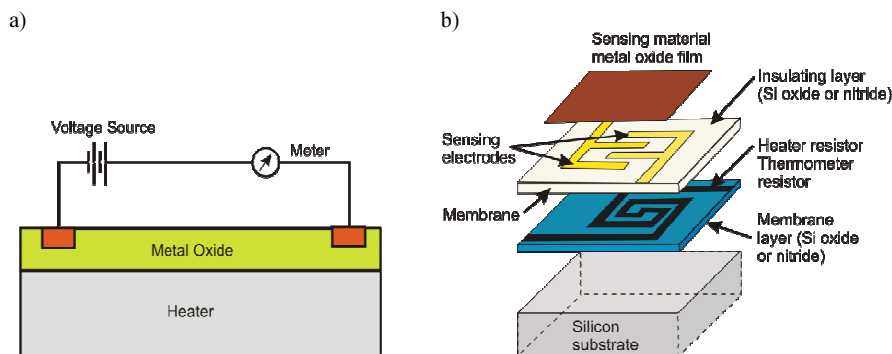


Fig. 5. a) The operation concept of a typical semiconductor gas sensor; b) an example of its construction.

Semiconductor gas sensors can be used in various applications ranging from safety equipment to emission control, air quality monitoring, and other measurement technologies. The main disadvantage is their limited sensitivity and selectivity. The DC resistance change is induced by the presence of various gases and humidity. Therefore, an array of resistive gas sensors of different properties has to be applied to determine the composition of gas mixtures. It means more expensive and bulky equipment, and extensive energy consumption.

Various methods can be applied to improve the gas sensing [15]. The most popular are the temperature modulation influencing the rate of adsorption/desorption processes [20], the modifications in the sensor construction, developing new sensor materials (*e.g.* Au nanoparticle gas sensors for VOC detection [21] nanoparticles increasing the gas sensing active area [22, 23]) or introducing catalytically active additives by bulk doping and surface modification [24].

Gas sensing can be also improved by UV light when the sensing layer exhibits the photocatalytic effect (*e.g.*  $\text{TiO}_2$ ,  $\text{WO}_3$ ) [15, 25, 26]. Application of UV light means that the

sensor operates in a lower temperature and that the response time can be also reduced. Moreover, UV light of different wavelengths can be generated by tiny and popular semiconductor diodes.

Another interesting method of improving the gas detection in resistive sensors was named the fluctuation enhanced sensing and was proposed by a few independent groups [27–29]. The method uses the low frequency resistance noise ( $1/f$ -like noise, typically in the frequency range below a few kHz) which depends on the gas ambient atmosphere. Measurements of low frequency noise give a better sensitivity because even small changes in the ambient gas can induce greater changes in the noise intensity. Moreover, noise is characterized by statistical functions (e.g. resistance fluctuation power spectral density) which provide more information than a single quantity (DC resistance only). Thus, we can simultaneously detect and determine the concentration of different gases using a single resistive gas sensor [30]. Such a method can be applied in relatively cheap gas detection systems using a microcontroller and a low noise voltage amplifier [31].

New materials have been continuously developed to improve sensors' characteristics. A good example are organically functionalized Au nanoparticles, because they can work at room temperature and can be very selective for various VOCs (e.g. formaldehyde, acetone, monoterpenes) [18]. It means that they are good candidates for economical and portable gas detection systems monitoring health by the breath analysis. We can suppose that such sensors will be continuously enhanced to reach the detection level of ppb and new gas detection systems as well as new detection methods will be proposed [32].

## 2.5. Surface Acoustic Wave gas sensor

*Surface Acoustic Wave* (SAW) sensors convert an input electrical signal onto a mechanical wave and measure its transmission through a sensing layer. There are different kinds of SAW sensors – some examples are presented in Fig. 6. The active layer – a receptor film – is placed on the transducer vibrating surface activated by an electronic device. When the sensor is exposed to an analyte, the receptor film properties (e.g. mass and thickness) change. It affects the frequency, amplitude and phase of the transmitted wave. The changes are proportional to the analyte concentration.

Recently, SAW sensors have been extensively used for detection of toxic chemical vapors [33]. They are applied to monitor gases and organic solvents using coating materials selectively adsorbing the molecules from air. The main advantages of this technology are: its high sensitivity, low power consumption, wireless, as well as the ability of operation in motion and in a hazardous environment. SAW devices are also technologically compatible with microelectronics, because the manufacturing processes of both are similar.

In practice, using SAW sensors the detection limit of 250 ppb for ammonia and 9 ppb for methane can be achieved [34].

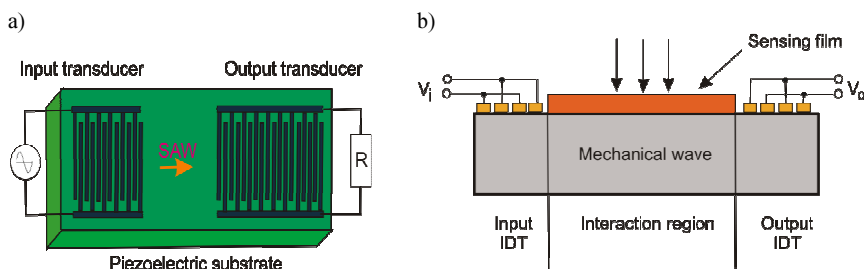


Fig. 6. a) The operation concept of a typical SAW gas sensor; b) its structure.



The devices described above provide an opportunity to detect a specific compound or group of compounds, therefore they are called sensors. A separate group of detection devices represent the gas analyzers. The most versatile one is the gas chromatograph. It enables examinations of volatile and semi-volatile compounds with a very high resolution. The main inconveniences of its application are the large size, high cost of purchase, expensive maintenance, and complicated operation.

### 3. Optical gas sensors – review

Optical methods of sensing trace matter are mostly based on absorption and emission spectrometry. However, in this paper, commonly used techniques based on measuring the optical absorption will be discussed. The operation principle of these techniques consists in detection of the gas concentration-dependent absorption of light at the specific wavelengths (so called fingerprints). For various compounds these wavelengths can be found in the HITRAN database [35]. The IR spectral range is particularly effective for gas detection. Analysis of the experimental results is based on the Beer-Lambert law.

Optical gas sensing methods have usually a higher sensitivity, selectivity and stability than the other ones. The methods include: *Non-Dispersive Infrared Spectroscopy* (NDIR), *Fourier Transform Infrared Spectroscopy* (FTIR), *Tunable Diode Laser Spectroscopy* (TDLAS), *Cavity Ring-Down absorption Spectroscopy* (CRDS), *Differential Optical Absorption Spectroscopy* (DOAS), *Differential Absorption Lidar* (DIAL), and *Photoacoustic Spectroscopy* (PAS).

#### 3.1. Non-Dispersive Infrared sensor (NDIR)

The NDIR sensor consists of an IR source, a gas cell, light filters and a photodetector (Fig. 7a). IR light is transmitted through the cell. If a specific component is present in the cell, the light absorption at the wavelengths defined by the active filter will be registered. The bandpass of the filter is matched to the fingerprint spectrum of the molecule of interest. In this way one minimizes the interference of measurement results caused by other compounds. The second detector, equipped with a filter matched to a not-absorbed wavelength, is used to determine a so-called measurement baseline. The concentration of molecules of interest might be calculated from both signals using the Lambert – Beer absorption law (Fig. 7b).

Jane Hodgkinson *et al.* showed that a short-term detection of noise equivalent concentration of 1 ppm CO<sub>2</sub> has been obtained [36].

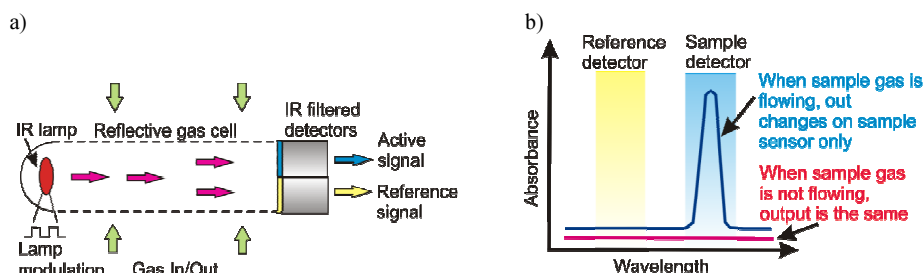


Fig. 7. a) A scheme of NDIR gas sensor [37]; b) registered photodetectors signals.

#### 3.2. Tunable Diode Laser Absorption Spectroscopy (TDLAS)

TDLAS spectroscopy is also known as *Wavelength Modulation Spectroscopy* (WMS). Its idea is presented in Fig. 8. The technique is used for detection of gas species using tunable



lasers. The laser wavelength is periodically modulated with a frequency  $f$  within the profile of absorption line of compound of interest:  $\lambda_L(t) = \lambda + \Delta\lambda\cos(2\pi ft)$ . Such a modulation induces the amplitude modulation of the light beam passing through the cell containing an absorber (Fig. 8a). The relevant periodical changes occur in the photodetector output signal which is then demodulated using a lock-in amplifier. When the wavelength  $\lambda$  is slowly scanned across the absorption line, the demodulation at frequency  $f$  provides the signal that is proportional to the first derivative of the line profile (Fig. 8b), while the  $2f$  – demodulation reveal the second derivative (Fig. 8c).

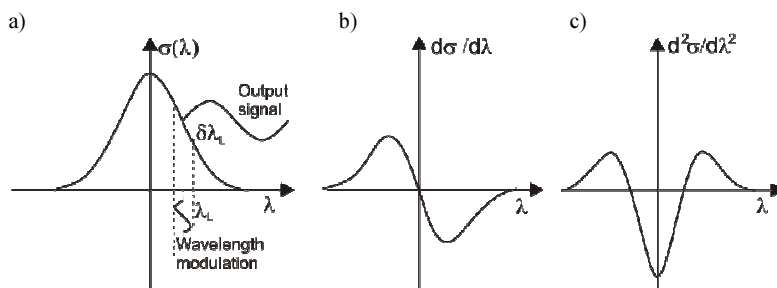


Fig. 8. The concept of TDLAS (WMS) spectroscopy ( $\sigma$  denotes the absorption cross-section).

The signal amplitude is proportional to the absorption coefficient. This approach improves selectivity and increases the detection process immunity to noise and interferences.

The TDLAS (WMS) setup consists of a tunable laser with a driving system, beam shaping optics, a gas probe, a photo-receiver with a signal processing unit (A/D), and a computer (Fig. 9a). Various approaches are applied: either one with stabilization of  $\lambda$  and  $\Delta\lambda$  parameters – which simply enables to determine the gas concentration, or another with registration of spectrum derivatives – which leads to better distinguishing the absorption lines in multicomponent media (Fig. 9b). TDLAS (WMS) provides an opportunity to detect the amount of substance fractions of gases from major to trace levels. This method is very selective and provides so-called *in situ* measurements. Using expression  $N = \alpha(\lambda)/\sigma(\lambda)$  (where  $N$  – concentration of the gas sample,  $\sigma(\lambda)$  – absorption cross-section and  $\alpha(\lambda)$  – absorption coefficient), the detection limit of TDLAS systems can be determined by the minimum detectable absorption coefficient at the level of  $10^{-4}$ – $10^{-6}$   $\text{cm}^{-1}$ .

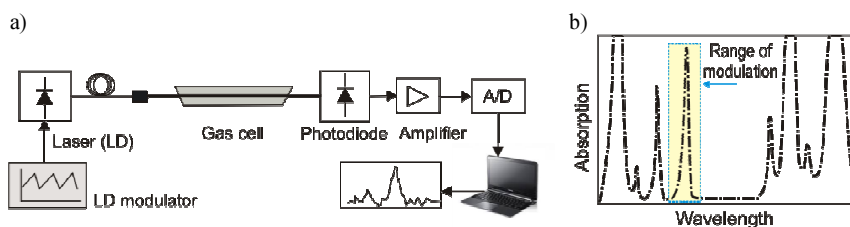


Fig. 9. a) A schematic diagram of TDLAS sensor; b) the absorption line.

Another experimental scheme of this approach for the mid-IR range with the use of quantum cascade lasers is presented in Fig. 10. In this case the method is called inter-pulse spectroscopy. This technique involves short current pulses with a superimposed sub-threshold ramp in order to tune the laser over a spectral line. It was pioneered by Namjou *et al.* [38] using 1 MHz series pulses with 11 ns duration and a ramp signal at the frequency of 4 Hz. That method ensured spectral tuning of each laser pulse with a slightly different wavelength



of about  $1\text{ cm}^{-1}$ . To obtain a higher frequency of temperature modulation, a combination of the ramp with a sinusoidal dither is usually applied. The spectral window of the analyses determined by inter-pulse tuning provides one-laser detection of several molecular species.

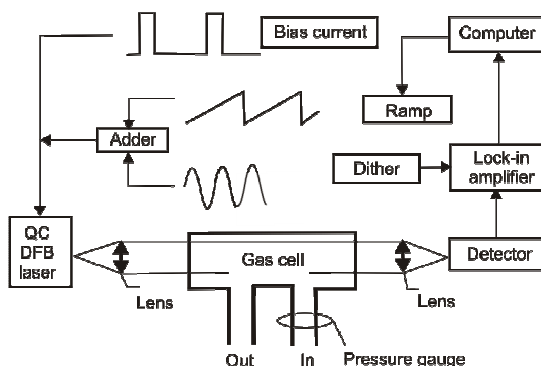


Fig. 10. A simplified scheme of the system for inter-pulse spectroscopy [38].

In practice, it is also possible to tune the laser spectra using longer pulses. It is applied in the intra-pulse modulation technique. In this technique, the laser is driven by a relatively long ( $\sim$  a few  $\mu\text{s}$ ) current pulse with the amplitude higher than the threshold value. During the current pulse, Joule heating causes a temperature change in the laser structure and spectral tuning of its radiation. The papers [39–42] describe the retuning process in the range of up to  $6\text{ cm}^{-1}$ . The tuning range depends on the pulse duration and system properties. The typical spectral resolution of this method is better than that of inter-pulse ones and is defined by the momentary laser line width. Its value is usually less than  $0.01\text{ cm}^{-1}$ . Fig. 11 presents a block diagram of the operating principle of intra-pulse method.

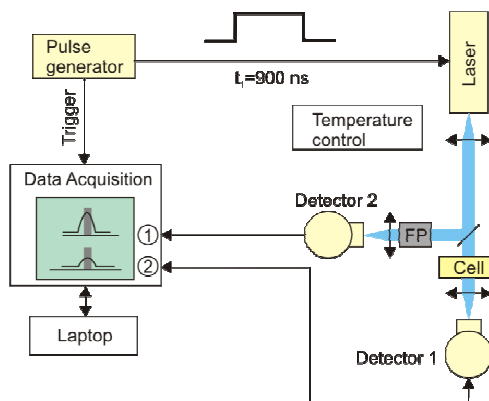


Fig. 11. A simplified scheme of the intra-pulse spectroscopy system [43].

### 3.3. Multipass Spectroscopy (MUPASS)

Optical trace detection of gas components requires a high sensitivity. The detection limit of commonly used single-pass spectrophotometry ( $\sim 10^{-4}\text{ cm}^{-1}$ ) is usually insufficient for this purpose. The high sensitivity can be achieved by lengthening the light path in the experimental cell containing the examined gas sample. Such an approach was employed in



multi-pass spectroscopy. The examined gas samples are contained in a cell built of two mirrors (Fig. 12). The light beam enters the cell through a hole in one mirror and then is reflected many times inside the cell. Due to that, its optical path is tens or even hundred times longer than that in single-pass spectroscopy. Such a solution results in a better detection limit reaching the value of  $\sim 10^{-7}$  cm $^{-1}$  (and even better). There are several kinds of this cell arrangement [1].

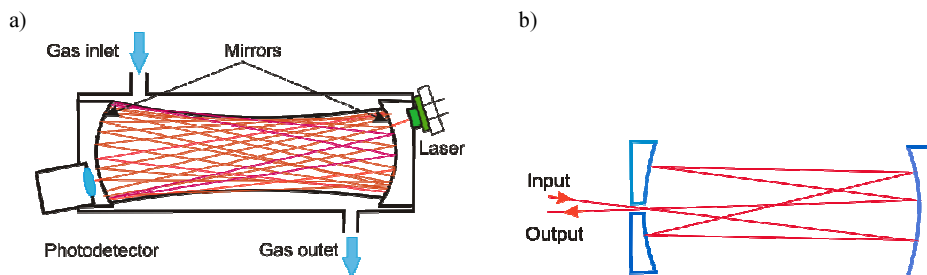


Fig. 12. a) The operation concept of White's; b) Herriott's multi-pass cells.

In White's cell (Fig. 12a), two special holes are made in surfaces of two mirrors. The first hole is aimed to let the light beam into the cell while the second one – to let it out. In Herriott's cell (Fig. 12b) the radiation is let in and out of the detector using the same hole. The optimal results are obtained for a special distribution of reflection points on the mirrors.

The MUPASS approach is often combined with the TDLAS (WMS) technique. Such a solution improves the sensor sensitivity and enables to measure lower gas concentrations. Fig. 13 shows an example of TDLAS technique with Herriott's cell. That system was used for measuring the NO concentration.

The laser was tuned within the range of 5.2105–5.2129  $\mu\text{m}$  by a ramp driving signal. The current pulses with 5 ms duration and 100 Hz repetition rate were used to set the laser temperature. Such a pulse length made the laser operate in the quasi-cw mode. To improve the signal to noise ratio, the absorption signals were averaged. The minimum detectable NO concentration was about 3 ppb.

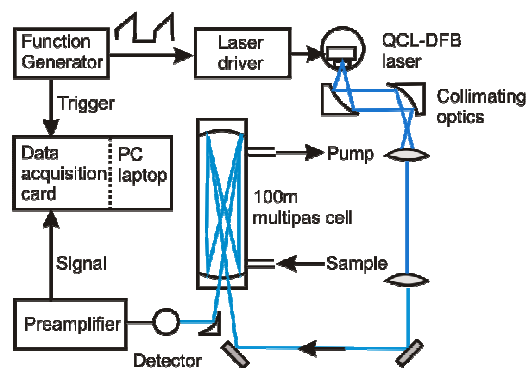


Fig. 13. A schematic of the TDLAS-MUPASS sensor [44].

Multipass spectroscopy used together with TDLAS (WMS) belongs to the most sensitive ones. This approach is useful for measurement of the absorption coefficients with a precision better than  $10^{-7}$  cm $^{-1}$ . Moreover, its maintenance is simple.

### 3.4. Differential Optical Absorption Spectroscopy (DOAS)

DOAS spectroscopy is used to measure concentrations of trace gases in the atmosphere. A simplified scheme of DOAS is shown in Fig. 14. Light from a broadband source (lamp) is collimated and sent to a receiver which is distant from about several hundred meters to several kilometers [45]. Therefore, this technique is capable to provide monitoring the atmospheric environment along the optical path. The lamp spectrum is modulated by extinction of air molecules and aerosols, as well as by many trace gases of different concentrations and absorption cross-sections. The received light is transmitted using an optical fiber to the spectrometer equipped with a computer. The absorption spectrum is compared with the reference one, which provides an opportunity to determine the concentration of trace gases.

A number of atmospheric species can be measured in the space using the DOAS method. They include pollutants such as ozone, nitrogen dioxide (NO<sub>2</sub>), sulfur dioxide (SO<sub>2</sub>), formaldehyde (CHCHO), carbon monoxide (CO), methane (CH<sub>4</sub>), and several other trace gases [46]. The detection limits of DOAS found in the literature (dependent upon a chosen system, path length, deployment configuration, and meteorological conditions) are from ppb to sub-ppb level (0.38 ppb – SO<sub>2</sub>, 0.5 ppb-NO<sub>2</sub>, 0.94 ppb-benzene) [47]. This technique is limited by interferences from other atmospheric components, such as rain, fog, or haze [48].

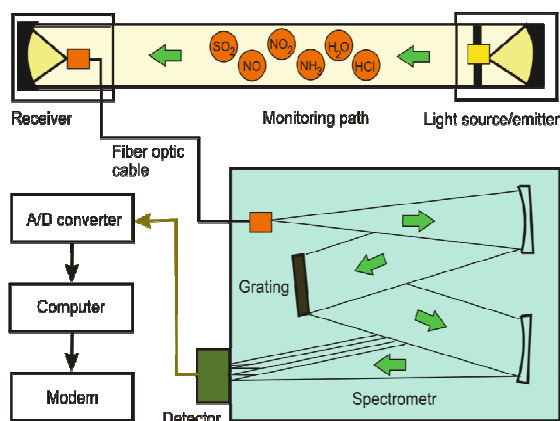


Fig. 14. A schematic of the DOAS sensor [49].

### 3.5. Differential Absorption Lidar (DIAL)

DIAL combines *Light Detection and Ranging* (LIDAR) and *Absorption Spectroscopy* technologies to identify and quantify the gas of interest (Fig. 15). In the single-wavelength LIDAR a laser source emits a light pulse with duration of a few nanoseconds. During the propagation of radiation the photons are scattered on aerosol and air particles. The backscattered light constitutes an echo signal which is registered by the lidar receiver, consisting of a telescope, a photodetector, and digitizing electronics. This signal is recorded as a function of time  $t$  with respect to the moment  $t_0$  of sending the laser pulse. These time-dependent data have a direct correspondence with the distance of the scattering position:  $z = c(t - t_0)/2$ , where  $c$  denotes the light speed. Such simple lidars are used for various applications, mainly for determining the aerosol distribution in atmosphere [50–53].

DIAL operates at two wavelengths. The first probing beam is matched to the molecular absorption line of the detected gas. The second one is out-tuned from the resonance and is used to determine the signal baseline. Analysis of both signals and knowledge of the absorption cross-section [54] provides an opportunity to determine the spatial distribution of concentration of the compound of interest.

The DIAL system presented by R. Robinson *et al.* [55] is prepared for detection of light hydrocarbons within 10 ppb to 100 ppb range, and 0.63 ppm of propane at the optical path of 1800 m. The DIAL system working on UV wavelengths was used by the University of Warsaw for remote examination of ozone, NO<sub>2</sub> and SO<sub>2</sub> conversion in atmosphere under various processes [56, 57]. The detection limits of 5 ppb were achieved. While in the infrared spectral range, specialists from the Military University of Technology designed a DIAL system for detection of methane with the detection limit of 50 ppm-m (parts per million times meter) [58].

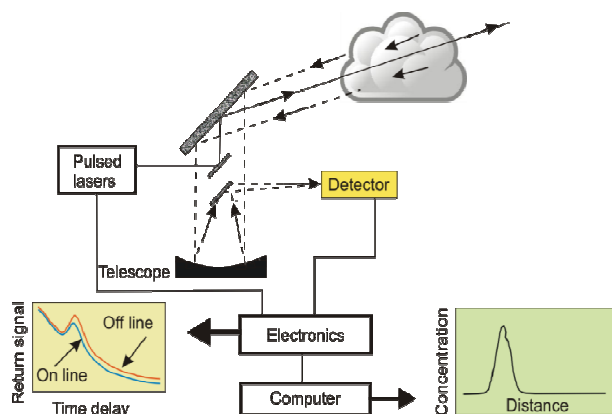


Fig. 15. The principle of determination of gas concentration and location by DIAL [55].

### 3.6. Photoacoustic Spectroscopy (PAS)

PAS spectroscopy is a powerful technique to measure concentrations of gases in the range from ppb to even ppt. PAS operation is based on conversion of a modulated light into a sound wave in the absorbing materials. The sample gas is injected into a photoacoustic chamber and irradiated with optical radiation. The wavelength corresponds with the absorption line of a molecule of interest. If an absorber is present in the chamber, a portion of optical radiation is converted onto heat energy. Then a local growth of the pressure and temperature occurs. When the optical beam is modulated with a certain frequency, it results in an acoustic wave. The strongest effect is achieved when the modulation frequency is matched to the resonance of the photoacoustic chamber. The acoustic wave is converted onto an electric signal with a high-sensitive microphone (Fig. 16). The microphone output signals are recorded using lock-in voltmeters.

A very high detection sensitivity can be achieved in the *Quartz Enhanced Photoacoustic Spectroscopy* (QEPAS). The principle of operation is similar to that of the PAS technique but the laser beam is focused between the teeth of a resonant piezo-quartz fork [60]. Such a transducer is sensitive to the signals generated by asymmetric tooth oscillations induced by the laser-stimulated acoustic wave. The signals from symmetric oscillations generated by external interfering sources are quenched. This feature as well as a high quality factor of the quartz fork results in an opportunity to construct ultra-compact sensors with a detectable concentration limit reaching the levels of a few ppb or even sub-ppb. In QEPAS setups, the

measurements are usually performed with a wavelength modulation technique using the  $2f$  detection [61].

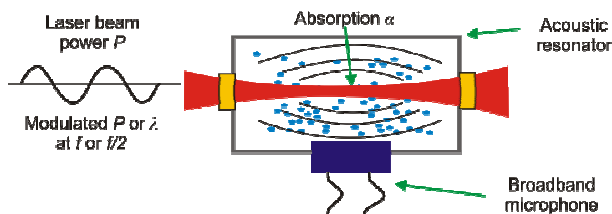


Fig. 16. The concept of photoacoustic spectroscopy [59].

### 3.7. Fourier Transform Infrared (FT-IR) spectrometry

The principle of FT-IR results from properties of the Michelson interferometer. Its scheme is presented in Fig. 17. When sliding of the mirror is performed, the Michelson interferometer produces a time-dependent signal which corresponds with the Fourier transform of light source spectrum (called interferogram) (Fig. 17a). During FT-IR operation, radiation from the source passes through the experimental cell, where the source spectrum is modified by the absorption of a sample. Then the interferogram is converted onto the transmission spectrum by computing the Fourier transform of the signal (Fig. 17b). FT-IR enables performing a precise measurement of the spectrum, increasing the speed (collecting a scan every second), and growing the sensitivity (averaging spectra to minimize random noise). Moreover, this method creates a wide spectrum of the sample covering simultaneously several molecular fingerprints reducing the scan time from several minutes (for common spectrography) to a few seconds.

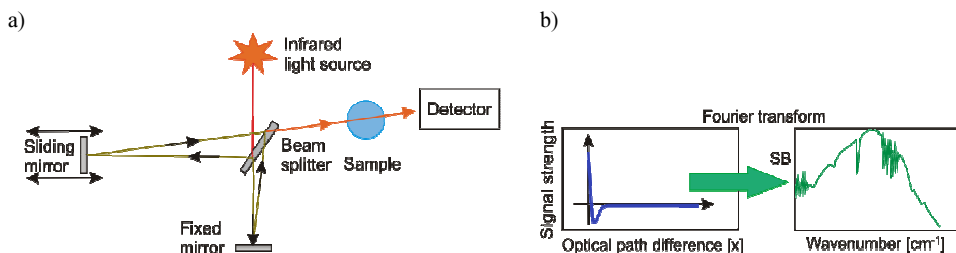


Fig. 17. a) The concept of FT-IR spectrometry; b) the interferogram of Fourier transformation.

### 3.8. Cavity Ring-Down Absorption Spectroscopy (CRDS)

CRDS is a highly-sensitive laser absorption technique for the quantitative detection of atomic and molecular species. CRDS was first demonstrated by O’Keefe and Deacon in 1988 [62]. This technique enables to measure the absorption using a high-finesse stable optical cavity. The principle of this method is presented in Fig. 18. Laser pulses are injected into an optical cavity consisting of two spherical and high-reflection mirrors. Due to multiple reflections the radiation can be stored inside the cavity. After each reflection, a small part of laser radiation leaves the cavity due to residual transmission of mirrors (Fig. 18). The

transmitted light decreases exponentially with the defined decay time often referred as the ring-down time.

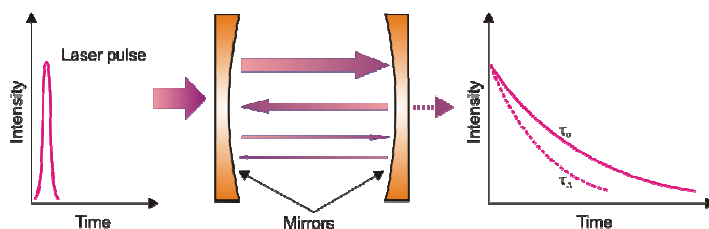


Fig. 18. The principle of CRDS.

When intrinsic cavity losses can be neglected, this decay time depends on the mirror reflectivity, resonator length, and extinction factor (absorption and scattering of light in the cavity) [63]. Then, determination of the absorption coefficient is possible by comparing the decay time values for the so-called “clear” cavity (reference value) with those for the cavity filled with the analyzed gas. The detection limit is related to the precision of decay time measurement.

Effective storage of light in the resonator is ensured only when the laser frequency is well matched to that of the cavity mode. Then, the best sensitivity can be achieved. However, the major disadvantage of this method is a strong dependence of the cavity mode frequency on mechanical instabilities causing fluctuations of the output signal [64]. Such disadvantages can be overcome using active stabilization of the cavity length [65, 66], or can be minimized with the CEAS approach – cavity enhanced absorption spectroscopy [67].

CEAS is based on the so-called off-axis arrangement of cavity. The radiation beam is injected under a small angle with respect to the cavity axis. As usually, the beam is repeatedly reflected by the mirrors; however, the reflection points are spatially separated. As the result, either a dense structure of weak modes is obtained or the modes do not occur. The system is much less sensitive to mechanical instabilities. The CEAS sensors attain the detection limit of about  $10^{-9} \text{ cm}^{-1}$  [68].

The detailed information about CRDS and CEAS techniques is presented in the authors’ papers [69–71].

#### 4. Experimental results

In this section some research activities in detection of three trace gas species in human breath (biomarkers) will be described. The main aim was to achieve substantial progress in early diagnosis of diseases owing to application of a low-cost and simply-maintained equipment for fast medical screening. In the designed instruments, optical techniques such as MUPASS and CEAS were applied. It was mentioned that laser absorption spectroscopy methods provide an opportunity to reach the trace gas detection limit of ppb level. However, during selection of the absorption spectra of some biomarkers, the main problem was to minimize the influence of other compounds (interferers), especially water and carbon dioxide. Their concentration in breath is much higher in comparison with the biomarkers’ threshold. Therefore, the art of selection of wavelengths and circumstances for optical detection of certain biomarkers consists in minimization of such interferences. That is why these spectroscopy methods require laser radiation that is precisely tuned to the peak of selected line. The laser linewidth and its fluctuations should be much lower than the absorption profile width.

#### 4.1. Nitric Oxide sensor

Monitoring the exhaled NO (FENO) is used to monitor asthma, hypertension, rhinitis and lung inflammation [72–74]. The nitric oxide level in human breath ranges from several ppb to several hundred ppb. Its fingerprint lines are located in the range of 5.260 – 5.266  $\mu\text{m}$ . Normally, the maximum of NO absorption corresponds with the wavelength of 5.263  $\mu\text{m}$ . However, this absorption line is strongly dominated by absorption bands of water vapor and carbon dioxide existing in the exhaled air. Reduction of H<sub>2</sub>O content by the factor of 30 using a dehumidifier is not able to eliminate its interferences. The solution consists in reduction of the breath sample pressure which causes a decrease of spectral lines broadening. Such line narrowing (with maintaining their amplitudes) provides splitting of NO specific absorption fingerprint from interferences caused by CO<sub>2</sub> and H<sub>2</sub>O.

The designed NO sensor consists of a laser with the control system, an optical system, a sample module and a signal processing unit. A high detection performance of the sensor is obtained by matching the quantum cascade laser wavelength to the NO absorption line (5.2630  $\mu\text{m}$ ). The optical cavity was built of two concave dielectric mirrors, 60 cm apart, 0,995 reflectivity at the wavelength of interest. The leakage radiation from the cavity was registered with optimized detection modules – PVI-2TE (VIGO System S.A.). The signal from the module was digitized using an AD converter (C328 series from Cleverscope). A precise laser current driver and a temperature controller (in the laser control system) ensured high stability of generated wavelengths.

The concentration of NO was calculated using special software. During examination of the NO sensor, the reference gas mixtures were delivered to the sensor at the atmospheric pressure and at the temperature of 296 K. The mixtures were prepared as biomarker signatures using a KIN-TEK generator of the gas standards. Owing to that, a high precision of the gas mixtures was ensured. The obtained results showed that the sensor provides the detection limits of 30 ppb. According to the ATS recommendation, NO concentrations higher than 50 ppb for adult patients and higher than 35 ppb for children, can be symptoms of atopic asthma, eosinophilic bronchitis or COPD with mixed inflammatory phenotype [75, 76]; therefore, the sensor can be used for the statement of morbid state in both cases.

#### 4.2. Carbon oxide and methane sensors

Looking for cheap solutions suitable for screening examination, it is reasonable to construct optical sensors working in the near-infrared range. In this range, one can expect a lower sensitivity in comparison with mid-infrared wavelengths, but still sufficient for effective monitoring several biomarkers in human breath. A profit consists in easily available and relatively cheap diode lasers, photodetectors (the photodiodes, much more sensitive than for the MIR spectral range), and standard optics. The compounds that occur in breath in relatively high concentrations are the most suitable for the NIR range. Carbon monoxide and methane belong to these biomarkers.

Carbon monoxide is a biomarker of hyper-bilirubin, oxidative stress, respiratory infections, and asthma [77–81]. It is also used to monitor bilirubin production in smoking cessation and access the lung diffusion capacity. The CO concentration in a healthy man breath should not exceed the value of 10 ppm, nevertheless in some cases (for smokers) it can reach 20 ppm [82]. The absorption line of 2.33372  $\mu\text{m}$  is the best candidate: the CO absorption coefficient at 10 ppm reaches here the value of  $4.4 \cdot 10^{-6} \text{ cm}^{-1}$ ; the interference of water vapor is about 200 times weaker and that of CO<sub>2</sub> is negligible.

The average concentration of methane in the exhaled air is about 3–8 ppm, but the upper limit should not exceed 10 ppm for a healthy man. The excess has been identified as a



biomarker of colonic fermentation and intestinal problems [83]. It was found that the wavelength of 2.25366  $\mu\text{m}$  with the absorption coefficient of  $1.25 \cdot 10^{-6} \text{ cm}^{-1}$  for 10 ppm is very suitable for detection of methane in breath. At this wavelength the interferences of both  $\text{CO}_2$  and  $\text{H}_2\text{O}$  are more than three orders of magnitude smaller.

Relatively high absorption coefficients of  $\text{CO}$  and  $\text{CH}_4$  at morbid state suggested applying the MUPASS technique together with WMS for their detection. Single-mode cw DFB-diode lasers tuned to respective absorption lines of the biomarkers were used. The triangle-shaped modulation of laser diode current enabled periodic scanning of wavelength over the absorption lines. The observation was performed when the scanning was done from the line peak to its right wing, (*i.e.* within the range of 2.25366–2.2537  $\mu\text{m}$  for  $\text{CH}_4$  and 2.336–2.33372  $\mu\text{m}$  for  $\text{CO}$ ).

The MUPASS cell (White's design) was constructed with two metallic mirrors, 0.5 m apart. Their diameter was 2 inch, while the radius of curvature was 2 m. The light beam was reflected 30 times between the mirrors and then was focused on the photodiode, providing the signal to the lock-in amplifier. The demodulated signal was finally averaged over 60 s.

Good linear correlation between the data supplied by the gas mixing system and the sensor was observed for both detection setups within the concentration range of 0.4–100 ppm. The precision of the measurement was better than 0.1 ppm. That is sufficient for monitoring carbon monoxide and methane in human breath for both sick and healthy man [84].

## 5. Conclusion

The presented work describes some practical aspects of the gas detection. A few examples of the gas sensing technology are briefly presented. However, the main attention of these analyses is paid on optoelectronic sensors and laser absorption spectroscopy. The operation principles and performances of some methods are also shown. In the experimental part of this work, some efforts concentrated on construction of a simple optoelectronic sensor for optical detection of certain biomarkers in breath are presented. The main goal was to achieve substantial progress in early diagnosis of diseases due to application of a low-cost and simply-maintained equipment for fast medical screening. The final goal will be an instrument designated for use in medicine doctors' cabinets, clinics and consulting rooms. The aim is developing and implementing to the clinical practice an early-warning table-top system for real-time detection of diseases. Such an apparatus should be simple and cheap. Its sensitivity should meet the requirements for medical applications.

## Acknowledgements

The work presented in this paper is supported by the National Centre for Research and Development within the scope of Project No.: 179900 (PBS1/A3/7/2012).

## References

- [1] Bielecki, Z., Janucki, J. (2012). Sensors and Systems for the Detection of Explosive Devices – An Overview. *Metrol. Meas. Syst.*, 19(1), 3–28.
- [2] Hodgkinson, J., Tatam, R.P. (2013). Optical gas sensing: a review. *Metrol. Meas. Syst.*, 24(1), 1–59.
- [3] Dakin, J.P., Chambers, P. (2006). Review of methods of optical gas detection by direct optical spectroscopy, with emphasis on correlation spectroscopy. *Optical Chemical Sensors*, NATO Science Series II: Mathematics, Physics and Chemistry, 24, 457–477.
- [4] Bielecki, Z., Stacewicz, T. et al. (2015). Application of quantum cascade lasers to trace gas detection. *Bull. Pol. Acad. Sci., Tech. Sci.*, 63(2), 515–525.





- [5] Buszewski, B., Grzywinski, D., *et al.* (2013). Detection of volatile organic compounds as biomarkers in breath analysis by different analytical techniques. *Bioanalysis*, 5(18), 2287–306.
- [6] Li, T., Xu, L., *et al.* (2012). A high heating efficiency two beam microplate for catalytic gas sensors. *Proc. of the IEEE International Conference on Micro Electronic and Mechanical Systems MEMS*, Kyoto, Japan, 65–68.
- [7] <https://en.wikipedia.org/wiki/Pellistor>
- [8] Park, S.Ch., Yoon, S.I., Lee, Ch.I., *et al.* (2009). A micro-thermoelectric gas sensor for detection of hydrogen and atomic oxygen. *Analyst.*, 134, 236–242.
- [9] Hierlemann, A., Baltes, H. (2003). CMOS-based chemical microsensor. *Analyst.*, 128, 15–28.
- [10] Yunusa, Z., Hamidon, M.N., *et al.* (2014). Gas sensors: a review. *Sensors & Transducers*, 168(4), 61–75.
- [11] [http://www.versaperm.com/thermal\\_conductivity\\_sensor.php](http://www.versaperm.com/thermal_conductivity_sensor.php)
- [12] Ohira, S., Toda, K. (2008). Micro gas analyzers for environmental and medical applications. *Anal. Chim. Acta*, 619, 143–156.
- [13] de Graaf, G., Wolfenbittel, R. (2012). Surface micromachined thermal conductivity detectors for gas sensing. *Proc. of the IEEE International Instrumentation and Measurement Technology Conference (I2MTC)*, Graz, 13–16 May, 1861–1864.
- [14] [https://en.wikipedia.org/wiki/Electrochemical\\_gas\\_sensor](https://en.wikipedia.org/wiki/Electrochemical_gas_sensor)
- [15] Xiong, L., Compton, R.G. (2014). Amperometric Gas detection: A Review. *Int. J. Electrochem. Sci.*, 9, 7152–7181.
- [16] Jasinski, P., Suzuki, T., Anderson, H.U. (2003). Nanocrystalline undoped ceria oxygen sensor. *Sens Actuators B Chem.*, 95(1), 73–77.
- [17] Gwizdź, P., Brudnik, A., Zakrzewska, K. (2015). Hydrogen detection with a gas sensor array – processing and recognition of dynamic responses using neural networks. *Metrol. Meas. Syst.*, 22(1), 3–12.
- [18] Korotcenkov, G. (2013). *Handbook of gas sensor materials*. Springer: New York, 49–116.
- [19] Zakrzewska, K. (2001). Mixed oxides as gas sensors. *Thin solid films*, 391(2), 229–238.
- [20] Smulko, J., Trawka, M. (2015). Gas selectivity enhancement by sampling-and-hold method in resistive gas sensors. *Sens. Actuators. B Chem.*, 219, 17–21.
- [21] Nakhleh, M.K., Broza, Y.Y., Haick, H. (2014). Monolayer-capped gold nanoparticles for disease detection from breath. *Nanomedicine*, 9(13), 1991–2002.
- [22] Ederth, J., Smulko, J., *et al.* (2006). Comparison of classical and fluctuation-enhanced gas sensing with PdxWO3 nanoparticle films. *Sens. Actuators. B Chem.*, 113(1), 310–315.
- [23] Heszler, P., Ionescu, R., *et al.* (2007). On the selectivity of nanostructured semiconductor gas sensors. *Phys Status Solidi*, 244(11), 4331–4335.
- [24] Halek, G., Malewicz, M., Teterycz, H. (2009). Methods of selectivity improvements of semiconductor gas sensors. *Proc. of the International Students and Young Scientists Workshop on Photonics and Microsystem*, Wernigerode, 31–35.
- [25] Lentka, Ł., Smulko, J.M., Ionescu, R., Granqvist, C.G., Kish, L.B. (2015). Determination of gas mixture components using fluctuation enhanced sensing and the LS-SVM regression algorithm. *Metrol. Meas. Syst.*, 22(3), 341–350.
- [26] Comini, E., Cristalli, A., Faglia, G., Sberveglieri, G. (2000). Light enhanced gas sensing properties of indium oxide and tin dioxide sensors. *Sens Actuators B Chem.*, 65(1), 260–263.
- [27] Kish, L.B., Vajtai, R., Granqvist, C.G. (2000). Extracting information from noise spectra of chemical sensors: single sensor electronic noses and tongues. *Sens. Actuators. B Chem.*, 71(1), 55–59.
- [28] Dziedzic, A., Kolek, A., Licznarski, B.W. (1999). Noise and nonlinearity of gas sensors – preliminary results. *Proc. 22nd Int. Spring Seminar on Electronics Technology*, Dresden-Freital, 99–104.
- [29] Vidybida, A.K. (2003). Adsorption – desorption noise can be used for improving selectivity. *Sens. Actuators. A Phys.*, 107(3), 233–237.



- [30] Kotarski, M.M., Smulko, J. (2010). Hazardous gases detection by fluctuation-enhanced gas sensing. *FNL*, 9(04), 359–371.
- [31] Kotarski, M., Smulko, J. (2009). Noise measurement set-ups for fluctuations-enhanced gas sensing. *Metrol. Meas. Syst.*, 16(3), 457–464.
- [32] Osowski, S., Siwek, K., et al. (2014). Differential electronic nose in on-line dynamic measurements. *Metrol. Meas. Syst.*, 21(4), 649–662.
- [33] Matatagui, D., Fernandez M.J., Fornateca, J. (2012). Love-wave sensor array to detect, discriminate and classify chemical warfare agent simulants. *Sens. Actuators. B Chem.*, 175, 173–178.
- [34] Hao, H.C., Chiang, M.C., et al. (2013). Improved surface acoustic wave sensor for low concentration ammonia/methane mixture gases detection. *17th International Conference on Miniaturized Systems for Chemistry and Life Sciences*, Freiburg, Germany.
- [35] HITRAN Database
- [36] Hodgkinson, J., Smith, R., et al. (2013). Non-dispersive infra-red (NDIR) measurement of carbon dioxide at 4.2  $\mu\text{m}$  in a compact and optically efficient sensor. *Sens. Actuators. B Chem.*, 186, 580–588.
- [37] <http://www.azosensors.com/Article.aspx?ArticleID=544>
- [38] Namjou, K., Cai, S., et al. (1998). Sensitive absorption spectroscopy with a room-temperature distributed-feedback quantum-cascade laser. *Optics Letters*, 23(3), 219–221.
- [39] Szabra, D., Bielecki, Z., et al. (2012). Interpulse and intrapulse spectroscopy with tunable quantum cascade lasers. *Conference IOS 2012*, Szczyrk-Beskidy Mountains, 34.
- [40] Mikołajczyk, J., Szabra, D., et al. (2014). Control systems of quantum cascade lasers. *Conference KKE 2014*, Darłówko, 456.
- [41] Szabra, D., Mikołajczyk, J., et al. (2013). Control system for some quantum cascade laser applications. *Conference KKE 2013*, Darłówko, 327–332.
- [42] Szabra, D., Mikołajczyk, J., et al. (2014). Power supply systems for quantum cascade lasers. *Electronics: structures, technologies, applications*, 11, 50–53.
- [43] Szabra, D., Nowakowski, M., et al. (2013). Quantum cascade laser driving in optical spectroscopy. *Electrotechnical Review*, 89(9), 173–177.
- [44] Menzel, L., Kostrev, A.A., et al. (2001). Spectroscopic detection of biological NO with a quantum cascade laser. *Appl. Phys. B*, 72(7), 859–863.
- [45] Yoshii, Y., Kuze, H., Takeuchi, N. (2003). Long-Path Measurement of Atmospheric NO<sub>2</sub> with an Obstruction Flashlight and a Charge Coupled Device Spectrometer. *Applied Optics*, 42, 4362–4368.
- [46] Richter, A. (2006). Differential optical absorption spectroscopy as a tool to measure pollution from space. *Spectroscopy Europe*, 18(6), 14–21.
- [47] <https://clu-in.org/programs/21m2/openpath/uv-doas/>
- [48] Committee on Monitoring at Chemical Agent Disposal Facilities, Board on Army Science and Technology, Division on Engineering and Physical Sciences, National Research Council. Monitoring at Chemical Agent Disposal Facilities. Washington, USA (2005).
- [49] <http://opsis.se/Products/MonitoringMethods/UVDOASTechnique/tabid/1097/Default.aspx#sthash.56aE9t3d.dpuf>
- [50] Weitkamp, C. (2004). *Lidar – range resolved optical remote sensing of the atmosphere*. Springer.
- [51] Chudzyński, S., Ernst, K., et al. (1996). Lidar monitoring of the atmosphere. *Proc. SPIE*, 3188, 168–179.
- [52] Zwoździak, J., et al. (2001). Some results on the ozone vertical distribution in atmospheric boundary layer from LIDAR and surface measurements over the Kamiencyk Valley. *Atmos. Research*, 58, 55–70.
- [53] Markowicz, K.M., Zielinski, T., et al. (2012). Remote sensing measurements of the volcanic ash plume over Poland in April 2010. *Atmospheric Environment*, 48, 66–75.
- [54] Stelmaszczyk, K., Czyżewski, A., et al. (2000). New Method of Elaboration of the Lidar Signal. *Appl. Phys. B*, 70, 295–301.



- [55] Robinson, R., Gardiner, T., *et al.* (2011). Infrared differential absorption Lidar (DIAL) measurements of hydrocarbon emissions. *J. Environ. Monit.*, 13, 2213–2220.
- [56] Chudzyński, S., Czyżewski, A., *et al.* (2001). Observation of Ozone Concentration during the Solar Eclipse. *Atmos. Research*, 57(1), 43–49.
- [57] Stacewicz, T., Chudzyński, S., *et al.* (2003). Studies of physical processes in the Earth's atmosphere. *Radiat. Phys. Chem.*, 68(1,2), 57–63.
- [58] Gietka, A., Mierczyk, Z., Muzal, M. (2006). Optoelectronic system for remote detection of contaminations and atmosphere pollution. *Bulletin of the Military University of Technology*, LV(2), 21–36.
- [59] Wojtas, J., Tittel, F.K., *et al.* (2014). Cavity enhanced absorption spectroscopy and photoacoustic spectroscopy for human breath analysis. *Int. J. Thermophys.*, DOI: 10.1007/s10765-014-1586-4.
- [60] Kosterev, A.A., Bakhrin, Y.A., *et al.* (2002). Quartz-enhanced photoacoustic spectroscopy. *Opt. Lett.*, 27, 1902–1904.
- [61] Tittel, F.K., Dong, L., *et al.* (2012). Sensitive detection of nitric oxide using a 5.26  $\mu\text{m}$  external cavity quantum cascade laser based QEPAS sensor. *Proc. SPIE* 8268, DOI: 10.1117/12.905621.
- [62] O'Keefe, A., Deacon, D.A.G. (1988). Cavity ring-down optical spectrometer for absorption measurements using pulsed laser source. *Rev. Sci. Instrum.*, 59, 2544–2551.
- [63] O'Neill, H., Gordon, S.M., *et al.* (1988). A computerized classification technique for screening for the presence of breath biomarkers in lung cancer. *Clin. Chem.*, 34, 1613–1618.
- [64] Berden, G., Peeters, R., Meijer, G. (2000). Cavity ring-down spectroscopy. Experimental schemes and applications. *Int. Rev. Phys. Chem.*, 19(4), 565–607.
- [65] Cygan, A., Lisak, D., *et al.* (2011). Pound-Drever-Hall-locked, frequency-stabilized cavity ring-down spectrometer. *Rev. Sci. Instrum.*, 82, 063107-1–063107-12.
- [66] Cygan, A., Wójtewicz, S., *et al.* (2013). Spectral line-shapes investigation with Pound-Drever-Hall-locked frequency-stabilized cavity ring-down spectroscopy. *Eur. Phys. J. Spec. Top.*, 222, 2119–2142.
- [67] Engel, R., Berden, G., *et al.* (1998). Cavity enhanced absorption and cavity enhanced magnetic rotation spectroscopy. *Rev. Sci. Instrum.*, 69, 3763–3769.
- [68] Wojtas, J., Czyżewski, A., *et al.* (2006). Sensitive detection of NO<sub>2</sub> with Cavity Enhanced Spectroscopy. *Optica Applicata*, 36(4), 461–467.
- [69] Wojtas, J., Mikołajczyk, J., *et al.* (2011). Applying CEAS method to UV, VIS, and IR spectroscopy sensors. *Bull. Pol. Acad. Sci., Tech. Sci.*, 59(4), 1–10.
- [70] Stacewicz, T., Wojtas, J., *et al.* (2012). Cavity Ring Down Spectroscopy: detection of trace amounts of matter. *Opto-Electron. Rev.*, 20(1), 34–41.
- [71] Wojtas, J., Bielecki, Z., *et al.* (2012). Ultrasensitive laser spectroscopy for breath analysis. *Opto-Electron. Rev.*, 20(1), 77–90.
- [72] Birrell, M.A., McCluskie, K., *et al.* (2006). Utility of exhaled nitric oxide as a noninvasive biomarker of lung inflammation in a disease model. *Eur. Respir. J.*, 28, 1236–1244.
- [73] [https://www.google.pl/search?q=nafion+humidifier&ie=utf-8&oe=utf-8&gws\\_rd=cr&ei=QrR\\_Vr-GCsXYyAOgso7wDQ](https://www.google.pl/search?q=nafion+humidifier&ie=utf-8&oe=utf-8&gws_rd=cr&ei=QrR_Vr-GCsXYyAOgso7wDQ)
- [74] Wang, Ch., Sahay, P. (2009). Breath Analysis Using Laser Spectroscopic Techniques: Breath Biomarkers, Spectral Fingerprints, and Detection Limits. *Sensors*, 9, 8230–8262.
- [75] <http://www.thoracic.org/about/overview.php>
- [76] [http://www.ersnet.org/images/stories/pdf/ERS\\_Annual\\_report\\_1314.pdf](http://www.ersnet.org/images/stories/pdf/ERS_Annual_report_1314.pdf)
- [77] Vreman, H.J., Mahoney, J.J., Stevenson, D.K. (1995). Carbon monoxide and carboxyhemoglobin. *Adv. Pediatr.*, 42, 330–334.
- [78] Stevenson, D.K., Vreman, H.J. (1997). Carbon monoxide and bilirubin production in neonates. *Pediatr. Rev.*, 100, 252–259.



- [79] Applegate, L.A., Luscher, P., Tyrrell, R.M. (1991). Induction of heme oxygenase: a general response to oxidant stress in cultured mammalian cells. *Cancer Res.*, 51, 974–978.
- [80] Yamaya, M., Sekizawa, K., et al. (1998). Increased carbon monoxide in exhaled air of subjects with upper respiratory tract infections. *Am. J. Respir. Crit. Care Med.*, 158, 311–314.
- [81] Zayasu, K., Sekizawa, K., et al. (1997). Increased carbon monoxide in exhaled air of asthmatic patients. *Am. J. Respir. Crit. Care Med.*, 156, 1140–1143.
- [82] Thorpe, M.J., Moll, K.D., et al. (2006). Broadband cavity ringdown spectroscopy for sensitive and rapid molecular detection. *Science*, 311, 1595–1599.
- [83] Le Marchand, L., Wilkens, L.R. (1992). Use of breath hydrogen and methane as markers of colonic fermentation in epidemiologic studies: circadian patterns of excretion. *Environ. Health Perspect.*, 98, 199–202.
- [84] Stacewicz, T. Bielecki, Z. et al. (2016). Detection of disease markers in human breath with laser absorption spectroscopy. *Opto-Electron. Rev.* (to be published).

